Design of an Improved Interval Type-2 Controller Using FCM and Supervised Clustering Algorithms

Anup Kumar MALLICK*, Achintya DAS

Department of Electronics & Communication Engineering, Kalyani Government Engineering College, Kalyani, Nadia, 741235, India

anup.mallick@kgec.edu.in (**Corresponding author*), achintya.das123@gmail.com

Abstract: In the last few decades, the interval type-2 fuzzy controller has gained popularity in comparison with the type-1 fuzzy controller. This is due to the capability of the interval type-2 fuzzy controller to better handle uncertainty and imprecision. However, modeling an intervaltype-2 fuzzy controller brings about several hurdles. One of the challenges of the design of an interval type-2 fuzzy controller is the generation of the primary membership functions with the purpose of formulating the upper and lower membership functions. This paper proposes a technique by which two Gaussian primary membership functions are generated for an interval type-2 fuzzy set. The means for the Gaussian membership functions are generated by employing two clustering techniques, namely the standard fuzzy c-means clustering algorithm and a recently developed supervised clustering algorithm. The standard deviations of the Gaussian membership functions are optimally selected by using the differential evolution algorithm. Besides, the number of rules required for the proposed model is much smaller. The proposed controller is applied to an armature-controlled DC motor and the obtained simulation results are compared with those obtained for the conventional interval type-2 fuzzy controller. The robustness of the proposed controller is also checked by adding noise and an impulse disturbance during the simulation.

Keywords: Interval Type-2 controller, Fuzzy C-means Clustering, Differential Evolution, Armature-Controlled DC Motor, Robust Control, Optimal Control.

1. Introduction

The type-1 (T1) fuzzy set (FS) can model a system based on a single expert's knowledge. With the type-2 (T2) fuzzy set, introduced by Zadeh (1975) and pioneered by Mendel & John (2002), it is possible to accommodate the knowledge of several experts. In type-2 fuzzy systems, the membership functions (MFs) are themselves fuzzy instead of crisp as in type-1 fuzzy sets. Although T2 fuzzy sets possess better handling capabilities for uncertainties and imprecision, their real-world applications require complex practical considerations (Wu & Mendel, 2019). As an intermediate solution, the more practical model for handling uncertainties is the interval type-2 (IT2) fuzzy set. In interval type-2 fuzzy sets, the membership is an interval instead of T1 fuzzy sets as in traditional generalized type-2 fuzzy sets. In the recent past, the modeling of control systems using IT2 FS has attracted increased interest from the research community.

Liang & Mendel (2000) described the theory and the design steps for an interval type-2 fuzzy logic system. Several researches and applications for the IT2 controller were followed thereafter. Wu & Tan (2004) proposed a singleton interval type-2 fuzzy controller to design the liquid-level control. An interval type-2 fuzzy sliding mode controller (IT2FSMC) is proposed in (Hsiao et al., 2008). IT2FSMC is a combination of the interval type-2 fuzzy logic control (IT2FLC) and the sliding-mode control (SMC) which shares the benefits of these two methods. IT2FSMC is used in many control applications, for example, to control a 3-DOF helicopter (Zeghlache et al., 2017), to control a robot manipulator (Nafia et al., 2018) and so on. Using a genetic algorithm, an optimal type-2 fuzzy controller is implemented for the velocity regulation of a DC motor in (Maldonado & Castillo, 2012). Behera et al. (2017) have applied an interval type-2 controller in the automatic generation control of a restructured power system. Control of a one-wheel vehicle in the real world has been developed using an adaptive interval type-2 fuzzy controller in (Chiu & Hung, 2020). Zakovorotniy & Kharchenko (2021) designed an optimal controller associated with speed control using the interval type-2 fuzzy set. The interval type-2 controller has also been designed based on the variations of the footprint of uncertainty. Zhou et al. (2021) have analyzed the variation trend of variable gains, in relation to the increase of footprint of uncertainty. Şahin & Ulu (2023) have proposed an IT2 controller with a dynamic footprint of uncertainty. The dynamic footprint of uncertainty has been defined as a function of system error. In (Şahin & Ulu, 2023), the IT2 controller with the dynamic footprint of uncertainty has been applied for controlling the altitude of a quadcopter.

One of the important tasks of an interval type-2 fuzzy set is to generate multiple type-1 fuzzy sets and then generate the upper and

https://doi.org/10.24846/v32i3y202308

lower membership functions from these type-1 membership functions by using some fuzzy operations. Similarly, an interval type-2 fuzzy logic controller should incorporate multiple type-1 fuzzy control strategies for the construction of the upper and lower membership functions. However, most of the IT2 FLC modeling found in literature either uses standard symmetrical equally spaced membership functions or the parameters of upper and lower membership functions are obtained by applying some optimization techniques. Not much attention is given to generating the primary membership functions to formulate the upper and lower membership functions. This paper addresses the above issue, and proposes a systematic method for generating two sets of membership functions for the interval type-2 controller. First, two primary membership functions are generated by using the clustering techniques and the differential evolution (Storn, 2008; Das & Suganthan, 2011) algorithm. Then, the upper and lower membership functions are generated by taking the fuzzy union and the fuzzy intersection of these two primary membership functions. This work addresses another challenge for interval type-2 controller, i.e., the number of rules. The proposed controller vividly reduces the required number of rules, thereby easing the computation. An armature-controlled DC motor is used to check the performance of the proposed controller. Noise and disturbance are added during simulation to check the robustness of the proposed controller. The remainder of this paper is structured as follows. Section 2 outlines the interval type-2 fuzzy sets and interval type-2 fuzzy logic controllers. Section 3 illustrates the proposed fuzzy controller. Section 4 provides the description of the applied process. The simulation results are presented and discussed in section 5. Section 6 includes the conclusion of this paper and refers to its possible future scope.

2. Preliminaries

2.1 Interval Type -2 Fuzzy Set

Unlike type-1 fuzzy sets, in IT2 FS (Mendel & Wu, 2010), each membership function consists of two MFs, i.e., upper membership function (*UMF*) and lower membership function (*LMF*). The area in the interval between the upper MF and the lower MF is called footprint of uncertainty (*FOU*). The *FOU* enables IT2 FS to represent the uncertainty in decision making. An example of an IT2 FS is shown in Figure 1 to indicate the different components of an IT2 FS.

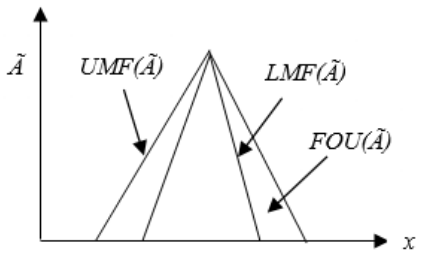

Figure 1. A schematic of an interval type-2 fuzzy set

The following definitions related to interval type-2 FS are used throughout the paper.

Definition 1[(IT2 FS)]

A T2 FS Ã is characterized by $\mu_{\tilde{A}}(x,m)$ and expressed by the following equation:

$$\tilde{A} = \int_{x\in X}\int_{m\in J_x} \mu_{\tilde{A}}(x,m)/(x,m) \qquad (1)$$

Here, X is the universe of discourse of the variable x, $m \in J_x \subseteq (0,1)$ is the primary membership value of x, and $\mu_{\tilde{A}}(x,m)$ denotes the secondary membership grade that is 1 for IT2 FS.

Definition 2 [(FOU)]

The *FOU* of $\tilde{A}$ is defined as the union of all of its primary MFs, and is expressed by equation (2):

$$FOU(\tilde{A}) = \cup_{\forall x\in X} J_x = (x,m); \quad \text{where } m \in J_x \subseteq [0,1]. \qquad (2)$$

Definition 3 [(Upper and lower MF)]

The upper bound of $FOU(\tilde{A})$ is called the *UMF* and is denoted by $\overline{\mu}_{\tilde{A}}(x)$. Similarly, the lower bound of $FOU(\tilde{A})$ is called *LMF* and is expressed by $\underline{\mu}_{\tilde{A}}(x)$. That is,

$$UMF = \overline{FOU(\tilde{A})} \quad \text{for} \quad \forall x \in X \qquad (3)$$

and

$$LMF = \underline{FOU(\tilde{A})} \quad \text{for} \quad \forall x \in X. \qquad (4)$$

2.2 Interval Type-2 Fuzzy Logic Controller

An interval type-2 fuzzy controller comprises four major building blocks, i.e. a fuzzifier, an

inference engine, a type reducer, and a defuzzifier (Chakraborty et al., 2015). A block diagram of an IT2 fuzzy logic controller (FLC) is shown in Figure 2.

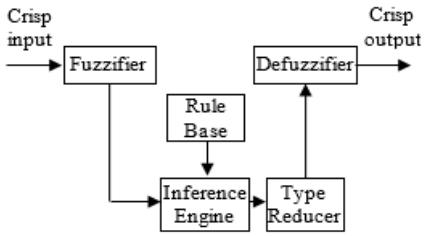

Figure 2. Block diagram of an interval type-2 FLC

3. The Proposed Interval Type-2 Controller

The proposed interval type-2 fuzzy controller is developed in the following three stages, namely generation of membership functions, formation of a fuzzy inference engine, and defuzzification.

3.1 Generation of Membership Functions

The common membership functions used in FLCs are the Gaussian, triangular, and trapezoidal one. For the proposed IT2 controller, the Gaussian membership functions are considered for two reasons. First, the Gaussian membership function requires a lower number of parameters in comparison with other membership functions. Secondly, the proposed controller generates membership functions based on traditional and an improved fuzzy c-means clustering, and the shape of the Gaussian function features a higher suitability or proximity to the FCM-like clustering algorithm. Two MFs are generated for each subset of antecedents and the consequence. A detailed step-by-step description of the membership functions` generation is provided below.

3.1.1 Generation of Control Surface

The control surface consists of error (*e*), change of error (Δ*e*), and control action (*u).* The MFs of e, Δ*e* and *u* are defined in the common interval of [-1, 1] as it is shown in Figure 3. This is one of the unbiased & natural ways of MF distribution.

The input space (*e,* Δ*e*) is uniformly sampled in 1,000 points in the interval of [-1, 1].

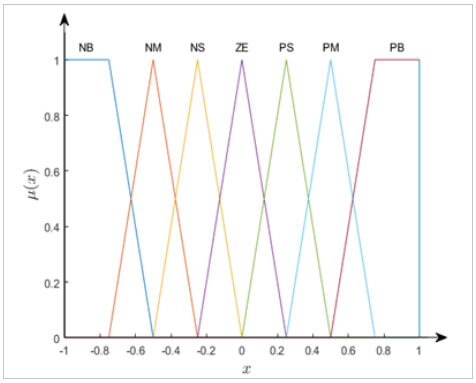

Figure 3. Membership functions of *e*, Δ*e* and *u* with NB: negative big, NM: negative medium, NS: negative small, ZE: zero, PS: positive small, PM: positive medium, and PB: positive big

Then the respective control actions for the sampled input space are calculated by the modified version of the original MacVicar-Whelan rule base (MacVicar-Whelan, 1976) with the 7 linguistic variables listed in Table 1.

Table 1. Rule base for generating the control action

Δ*e*/*e*	NB	NM	NS	ZE	PS	PM	PB
NB	NB	NB	NB	NM	NS	NS	ZE
NM	NB	NM	NM	NM	NS	ZE	PS
NS	NB	NM	NS	NS	ZE	PS	PM
ZE	NB	NM	NS	ZE	PS	PM	PB
PS	NM	NS	ZE	PS	PS	PM	PB
PM	NS	ZE	PS	PM	PM	PM	PB
PB	ZE	PS	PS	PM	PB	PB	PB

By combining, [e, Δe] with the control action u obtained in Table 1, a control surface is generated as it is illustrated in Figure 4.

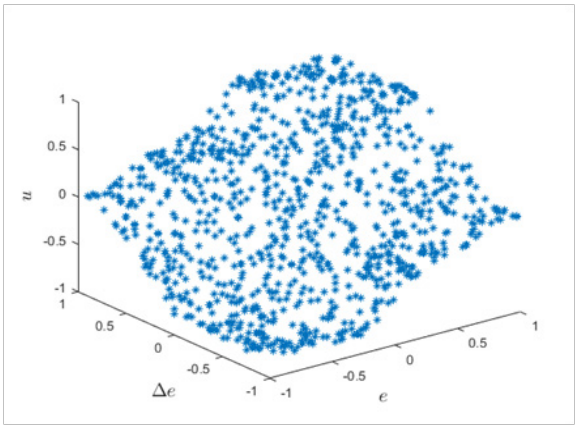

Figure 4. The generated control surface

3.1.2 Clustering of the Control Surface

Next, the control surface is clustered into *c* number of clusters. As each process input *e* and Δe can be divided into 3 major groups, i.e. negative, zero, & positive, c is selected as 3*3=9 to cover the control surface significantly. The control surface is first clustered into 9 groups by traditional fuzzy c-means clustering. It provides one set of means for the Gaussian membership functions. A second set of cluster centers is obtained by using a newly developed supervised clustering algorithm. The details on supervised clustering can be found in (Bandyopadhyay et al., 2007; Mukhopadhyay & Maulik, 2009). The two major steps of supervised clustering are to first segregate the core and boundary data points, and then to apply supervised learning in clustering. From the membership matrix of FCM, the membership values of the data points for all the clusters are found. Among the membership values of a data point for all the clusters, let us assume that the highest membership of a data point (x_i) is represented by μ_{hi} and the second highest membership is denoted by μ_{nhi}, and the difference between these two membership values is represented by $\Delta\mu_i$. Data points with a higher $\Delta\mu_i$ are assumed to be near a cluster center and are designated as core data points. On the other hand, the data points with a lower $\Delta\mu_i$ are considered to be at the overlap of at least two clusters and are defined as boundary data points. The membership-related threshold for deciding if a data point belongs either to the core data set or to the boundary data set plays a significant role in the final cluster solution. Mallick & Mukhopadhyay (2018) proposed a scheme, namely *Clusterwise mean* to separate the core data points and boundary data points. In *Clusterwise mean*, the core data set is formed by taking core data points from each cluster. Hence, the membership-related threshold is selected cluster-wise. In this method, the threshold of a cluster is the mean value of membership differences $\Delta\mu_i$ for all the data points belonging to that cluster only, and is determined by equation (5).

$$\Delta\mu_{threshold}(j) = \frac{1}{n_j}\sum_{p\in C_j}\Delta\mu_p \tag{5}$$

Here, C_j denotes the j^{th} cluster, n_j is the number of data points in j^{th} cluster, p is the index of data points belonging to j^{th} cluster, i is a set given by $\{1,2,3,\ldots,n\}$, and n is the number of all data points. The data points with $\Delta\mu_i \geq \Delta\mu_{threshold}$ of that cluster are regarded as core data. The overall core data set is formed by amalgamating the core data points coming from each cluster. After the segregation of core and boundary data points, the class labels of the boundary data points are predicted by a *k-nn* classifier based on the class labels of the core data points. In this paper, the value of *k* in the *k-nn* classifier is set to 5. The final cluster centers are found by averaging the data points belonging to that cluster. The cluster centers obtained by traditional FCM and by *Clusterwise mean* provide two sets of means for the primary Gaussian membership functions.

3.1.3 Selection of the Standard Deviations of the Primary MFs

The standard deviations of the Gaussian membership functions are optimally selected by differential evolution (DE). Here, each chromosome consists of 27 genes (9 genes for the standard deviation of the *e* component, the next 9 genes for the Δe component, and the last 9 genes for the *u* component). In each run, DE optimizes the value of standard deviations by minimizing the sum of squared errors (SSE) of the data points of the control surface.

$$SSE = \sum_{i=1}^{k1}(act(u_i) - est(u_i))^2 \tag{6}$$

Here, *k1* is the number of data points, *est(u)* is the estimated control action for a population with a certain set of standard deviations, and *act(u)*is the output found from the control surface. The best solution found at the last iteration of DE is translated as the standard deviations of the respective Gaussian MFs. The pseudo-code of the differential evolution algorithm used here is given in Algorithm 1.

3.1.4 Formation of *UMF* and *LMF*

As the control surface is clustered into 9 groups, each antecedent (e, Δe), and consequence (u) consist of 9 membership functions. Two sets of primary Gaussian MFs for the antecedents and the consequence are formed by considering cluster centers as the means, and the solution of differential evolution as the standard deviations. These two Gaussian membership functions shall be defined as *GMF1* and *GMF2*. Then the upper membership functions (*UMFs*) are generated by using the fuzzy MAX operation over *GMF1* and *GMF2* as it is given in equation (7).

$$UMF = \max_{\forall i}\ \mu_{GMF1}(x(i)), \mu_{GMF2}(x(i)) \quad \text{for} \quad \forall x \in X \tag{7}$$

Algorithm 1: Pseudocode to generate standard deviations of the Gaussian MFs

Require: Control surface data, *popsize*, *Maxiter*, means of the Gaussian MFs

Ensure: Standard deviations of the Gaussian MFs

Randomly generate initial population $x_{i,G}$; i =1, 2, ..., *popsize*

Evaluate cost $f(x_{i,G})$ using procedure *SSE*

Find the best population *pbest* of the population $x_{i,G}$

$G \leftarrow 0$

while $G <$ *Maxiter* ***do***

  G ← G + 1

  for *i = 1 to popsize* ***do***

    Select randomly *r*1 and *r*2 such that $i \neq r1 \neq r2$

    Generate F from normal distribution

$$v_{i,G+1} = x_{i,G} + F*\left(pbest - x_{i,G} + x_{r1,G} - x_{r2,G}\right)$$

    Calculate cost $f(v_{i,G+1})$

    if $f(v_{i,G+1}) < f(x_{i,G})$ ***then***

      $x_{i,G+1} = v_{i,G+1}$

      else $x_{i,G+1} = x_{i,G}$

    end

  end

  Find the *pbest* of the population $x_{i,G+1}$

end

Procedure *SSE(f)*

  Formulate UMF&LMF using Means and translating genes of the chromosome as the standard deviations

  Evaluate the estimated outputs (u) for all the input data points (e, Δe) of the control surface

  Calculate $f = \sum_{i=1}^{k1}\left(act(u_i) - est(u_i)\right)^2$;

  k1: no. of data points on the control surface

  Return f

End

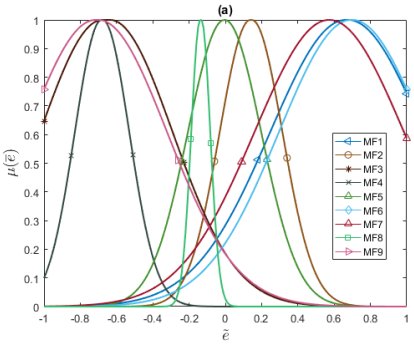

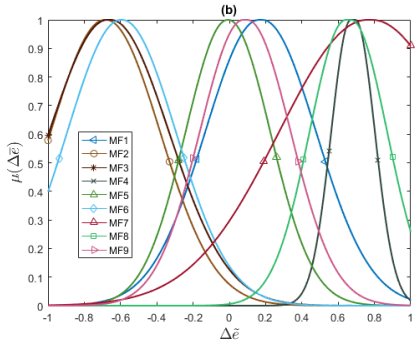

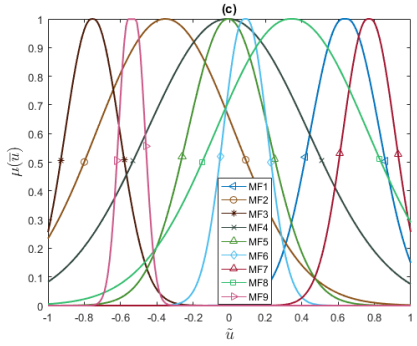

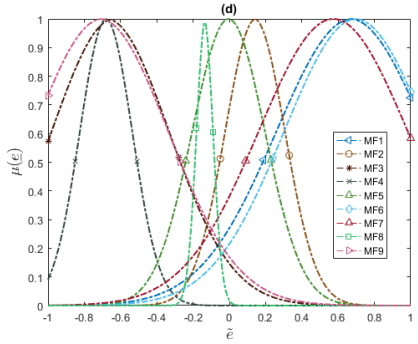

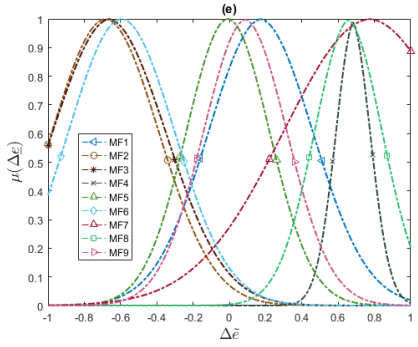

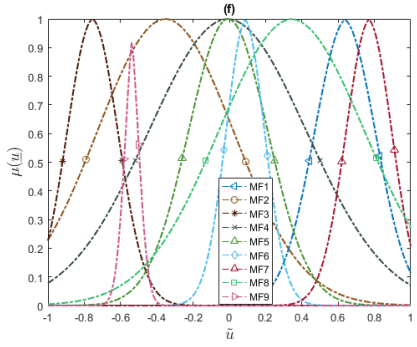

Figure 5. Membership functions (MFs) of the proposed IT2 FLC: *UMFs* of (a) error (*e*); (b) change of error (Δ*e*) and (c) control action (*u*); *LMFs* of (d) error (*e*); (e) change of error (Δ*e*) and (f) control action (*u*)

Similarly, lower membership functions (*LMFs*) are obtained by taking the minimum of *GMF1* and *GMF2* as in equation (8).

$$LMF = \min_{\forall i} \mu_{GMF1}(x(i)), \mu_{GMF2}(x(i)) \quad \text{for} \quad \forall x \in X \tag{8}$$

The upper and lower MFs obtained for the antecedents and the consequence of the proposed IT2 FLC are shown in Figure 5.

3.2. Fuzzy Inference System

Let us assume that the process input at an instant be denoted by e_{in} and Δe_{in}. The membership intervals of e_{in} are computed by means of projection of e_{in} to the e component of all the 9 rules. Similarly, the membership intervals of Δe_{in} are also calculated. Then the firing interval $[\underline{f}^k, \overline{f}^k]$ at k^{th} rule is estimated by *minimum t-norm*. In Example 1, the procedure of the fuzzy inference system is illustrated.

Example 1. Let the projections of e_{in} on the k^{th} *LMF* and k^{th} *UMF* be expressed by $fL1$ and $fU1$, respectively, and the positions of Δe_{in} on the k^{th} *LMF* and k^{th} *UMF* be expressed by $fL2$ and $fU2$, respectively. Then, the firing strength of *LMF* of k^{th} rule denoted by $\underline{f}^k$ is calculated as it is given in equation (9).

$$\underline{f}^k = \min(fL1, fL2) \tag{9}$$

Similarly, the firing strength of *UMF* of k^{th} rule expressed by $\overline{f}^k$ is estimated by equation (10).

$$\overline{f}^k = \min(fU1, fU2) \tag{10}$$

Next, the inferences due to firing of k^{th} rule are obtained from the intersection of $\underline{f}^k$ with $LMF_k(\tilde{u})$, and from the intersection of $\overline{f}^k$ with $UMF_k(\tilde{u})$. Let the consequence fuzzy output of *LMF* and *UMF* of k^{th} rule be denoted by LMF^k and UMF^k, respectively. Thus,

$$LMF^k = \min(\underline{f}^k, LMF_k(\tilde{u})) \tag{11}$$

and

$$UMF^k = \min(\overline{f}^k, UMF_k(\tilde{u})). \tag{12}$$

3.3. Defuzzification

The total output of *LMF* (and *UMF*) for a discrete output point is obtained by *MAX* aggression of all the rules. Let the output *LMF* and *UMF* at n^{th} data point be denoted by $\underline{r}^n$ and $\overline{r}^n$, respectively. Then,

$$\underline{r}^n = \max(LMF^1, ..., LMF^k, ..., LMF^N), \tag{13}$$

and

$$\overline{r}^n = \max(UMF^1, ..., UMF^k, ..., UMF^N), \tag{14}$$

where N is the total number of rules. Next, the fuzzy output is defuzzified. In this paper, the Nie-Tan method of defuzzification (Nie & Tan, 2008; Wu, 2012) was used. In this method, the crisp output y of an IT2 FLC is estimated by the following in equation (15).

$$y = \frac{\sum_{n=1}^{P} y_n(\underline{r}^n + \overline{r}^n)}{\sum_{n=1}^{P}(\underline{r}^n + \overline{r}^n)}, \tag{15}$$

where P is the number of output discrete points.

4. The Applied Process

The armature-controlled DC motor is widely used in many industrial applications. Hence, researchers still use DC motors as a process for validating their proposed controller (Sankeshwari & Chillé, 2019; Li et al., 2021). The block diagram of the armature-controlled DC motor is shown in Figure 6 and the transfer function of the armature-controlled DC motor is given by equation (16).

$$\frac{\theta_m(s)}{E_a(s)} = \frac{K_T}{JL_a s^3 + (R_a J + L_a B)s^2 + (R_a B + K_b K_T)s} \tag{16}$$

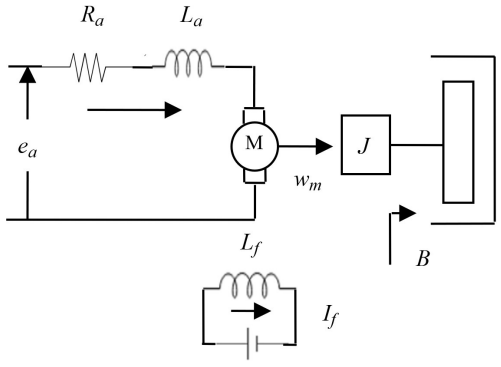

Figure 6. Block diagram of an armature- controlled DC motor

Here, θ_m: angular position of the motor shaft, ea: applied voltage, K_T: torque constant of motor, J: the moment of inertia, K_b: voltage constant of the motor, B: viscous friction coefficient, L_a: armature inductance, and R_a: armature resistance. In an armature-controlled DC motor, the armature inductance is negligibly small compared to armature resistance (Mandal, 2014). Thus,

the transfer function in equation (16) can be approximated as equation (17).

$$\frac{\theta_m(s)}{E_a(s)} = \frac{K_T / R_a J}{s^2 + (B/J + K_b K_T / R_a J)s} \quad (17)$$

5. Results and Discussion

For uniformity purposes, all the simulations were carried out by a fourth-order Runge-Kutta solver with a fixed interval of 0.01 seconds. In order to illustrate the performance of the proposed model, a conventional IT2 FLC is considered for comparison purposes. The membership functions of the conventional IT2 FLC are considered to be symmetrical triangles (except for the two MFs at the extreme ends) as it is shown in Figure 7. The simulation is done in Matlab R2016a for the block diagram shown in Figure 8. For an unbiased comparison, the values of all the gain parameters, namely G_e, $G_{\Delta e}$, and G_{PD} in Figure 8, were optimized using differential evolution (DE) for both the proposed model and for the conventional fuzzy logic controller. In DE, Integral square error (ISE) is considered as the objective function given in equation (18).

$$ISE = \sum_{i=1}^{nL} e^2(i), \quad (18)$$

where e(i) is the error, i.e. the difference between the desired step response and the actual step response at the ith discrete point for a set of [G_e, $G_{\Delta e}$, G_{PD}]; n is the number of discrete data points, and L is the sampling time, i.e. 0.01 seconds in this paper. Here, n is considered to be 3000, as after 3 seconds the fluctuation in the response reduces sufficiently. The algorithm of differential evolution used here for the optimized selections of the gain parameters is similar to Algorithm 1, except that the cost function is calculated using equation (18).

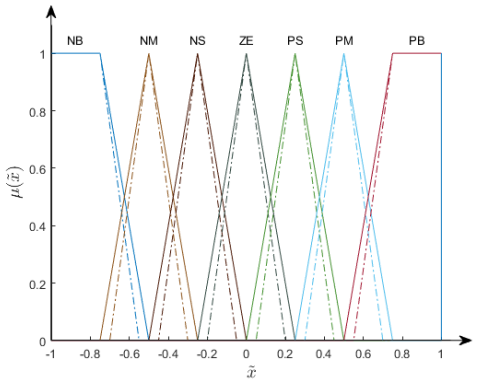

Figure 7. MFs of conventional IT2 controller; solid lines: *UMFs,* dashed lines: *LMF* of *e*/ Δ*e*/ *u*

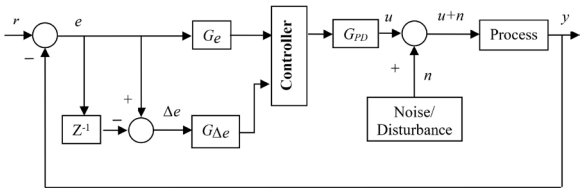

Figure 8. Matlab simulation block diagram

The value of R_a is set at 0.4 ohm, that of J at 0.5 kg-m2, that of K_b at 1.25 V-s/rad, the value of K_T at 1 N-m/A, and that of B at 0.01N-m/rad (Rahman, 2017). The simulation results for the step response with the conventional IT2 controller and with the proposed controller are shown in Figure 9(a) and in Figure 9(b), respectively. From Figure 9, it can be seen that the proposed IT2 controller has a faster response with a lower overshoot, and also settles earlier in comparison with the conventional IT2 controller. The robustness of the proposed controller is checked in two ways; by applying a random noise, and by adding a sudden impulse disturbance. The mean and the variance of the random noise are 0 and 0.1, respectively, and the applied disturbance is of 30-unit impulse.

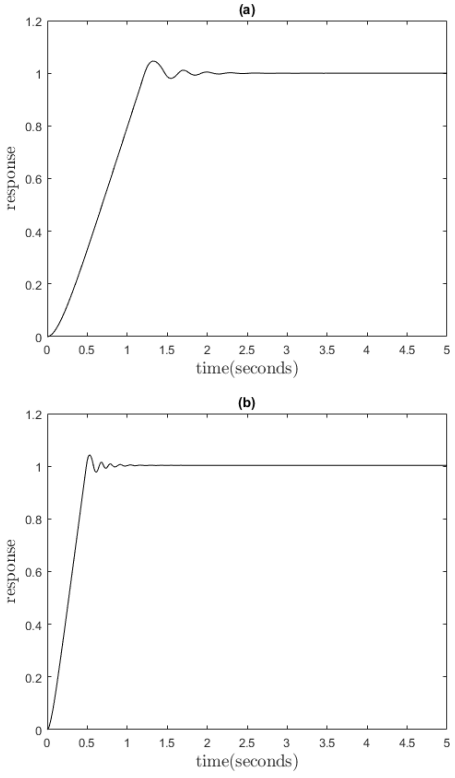

Figure 9. Step responses of the DC motor in the no noise and no disturbance conditions for (a) the conventional IT2 controller; (b) the proposed IT2 controller

The simulation results for the step response in the presence of the noise and disturbance are shown in Figure 10 and in Figure 11, respectively.

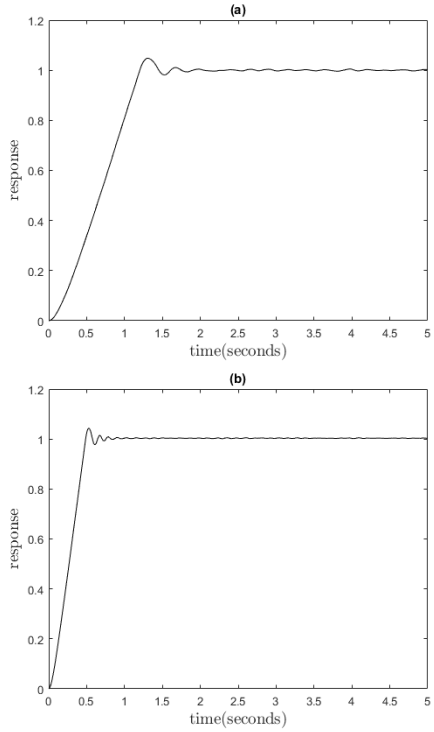

Figure 10. Step responses of the DC motor in the presence of random noise with a variance of 0.1 for (a) the conventional IT2 controller; (b) the proposed IT2 controller

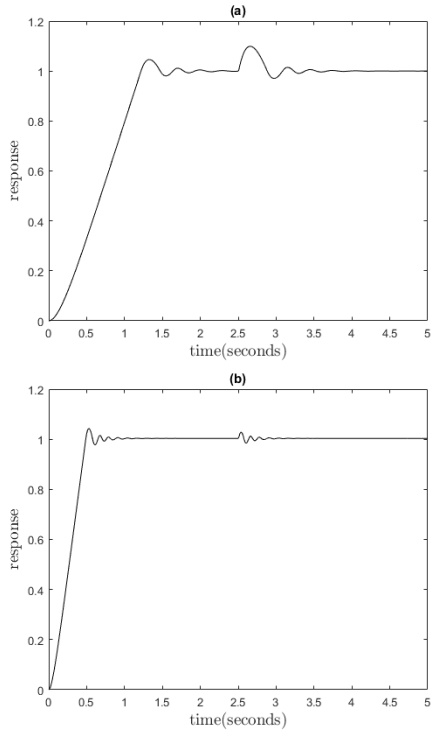

Figure 11. Step responses of the DC motor with 30-unit impulse disturbance applied at 2.5 seconds for (a) the conventional IT2 controller; (b) the proposed IT2 controller

From Figure 10, it appears that the fluctuation in response due to the random noise for the proposed controller is much lower than for the conventional controller. Figure 11 indicates that the proposed controller is more aggressive than the conventional controller at the event of disturbance. During the simulation, it was found that the conventional controller required 0.54 seconds, whereas the proposed controller takes only 0.06 seconds to settle after applying the disturbance. It was also seen that the proposed controller features a lower overshoot (2.81%) in comparison with an overshoot of 9.89% for the conventional controller due to the disturbance.

The values of different time domain performance indices, namely rise time (t_r), peak overshoot (M_p), settling time (t_{ss}), integral absolute Error (*IAE*), integral time absolute error (*ITAE*), integral square error (*ISE*), and integral time squared error (*ITSE*) are included in Table 2.

Table 2. Comparative performance of conventional and proposed IT2 controller

Noise/ Disturbance	Time domain performance index	IT2 Controller used	
		Conventional	Proposed
No noise and no disturbance applied	t_r (sec.)	1.22	0.49
	M_p%	4.59624	4.29711
	t_{ss} (sec.)	1.44	0.63
	IAE	0.68807	0.28447
	ITAE	0.29912	0.08630
	ISE	0.49016	0.19074
	ITSE	0.15704	0.02434
Random noise with a Variance of 0.1	t_r (sec.)	1.21	0.49
	M_p%	4.80191	4.28470
	t_{ss} (sec.)	1.42	0.63
	IAE	0.68119	0.28314
	ITAE	0.30557	0.08655
	ISE	0.48081	0.18938
	ITSE	0.15218	0.02408
Unit impulse disturbance applied at 2.5 seconds	t_r (sec.)	1.22	0.49
	M_p%	4.59624	4.29711
	t_{ss} (sec.)	1.44	0.63
	IAE	0.72002	0.28640
	ITAE	0.38856	0.09130
	ISE	0.49220	0.19079
	ITSE	0.16255	0.02445

From Table 2, it appears that the proposed IT2 controller outperforms the conventional

IT2 controller for all the performance indices considered here.

6. Conclusion and Future Scope

This paper prescribes a systematic approach to modelling an interval type-2 fuzzy logic controller. It proposes a way to generate primary type-1 membership functions in order to formulate the upper and the lower membership functions for the interval type-2 controller. The number of rules is also reduced from 49 for the conventional IT2 controller to only 9 for the proposed IT2 controller. From the obtained simulation results, it can be seen that the proposed controller outperforms the conventional IT2 controller, and that it also shows robustness to the noise and the applied disturbance.

The present work considers the shape of primary membership functions as being Gaussian. Further research may also be conducted with the purpose of generating an IT2 controller with triangular or trapezoidal membership functions.

REFERENCES

Bandyopadhyay, S., Mukhopadhyay, A. & Maulik, U. (2007) An improved algorithm for clustering gene expression data. *Bioinformatics*. 23(21), 2859–2865. doi: 10.1093/bioinformatics/btm418.

Behera, A., Adhya, D. G. & Parida, S. K. (2017) Analysis of robust interval type-2 fuzzy PID controller for AGC in a restructured power system. In: 7th International Conference on Power Systems, December 21-23, Pune, India. pp. 168-174.

Chakraborty, S., Konar, A., Ralescu, A. & Pal, N. R. (2015) A fast algorithm to compute precise type-2 centroids for real-time control applications. *IEEE Transactions on Cybernetics*. 45(2), 340-353. doi: 10.1109/TCYB.2014.2308631.

Chiu, C. H. & Hung, Y. T. (2020) One wheel vehicle real world control based on interval type 2 fuzzy controller. *Mechatronics*. 70, 102387. doi: 10.1016/j.mechatronics.2020.102387.

Das, S. & Suganthan, P. N. (2011) Differential evolution: A survey of the state-of-the-art. *IEEE Transactions on Evolutionary Computation*. 15(1), 4-31. doi: 10.1109/TEVC.2010.2059031.

Hsiao, M.-Y., Li, T.-H. S., Lee, J.-Z., Chao, C.-H. & Tsai, S.-H. (2008) Design of interval type-2 fuzzy sliding-mode controller. *Information Sciences.* 178(6), 1696-1716. doi: 10.1016/j.ins.2007.10.019.

Li, J., Ma, K. & Wu, Z. (2021) Prescribed performance control for uncertain flexible-joint robotic manipulators driven by DC motors. *International Journal of Control, Automation and Systems.* 19, 1640-1650. doi: 10.1007/s12555-020-0311-2.

Liang, Q. & Mendel, J. M. (2000) Interval type-2 fuzzy logic systems: Theory and design. *IEEE Transactions on Fuzzy Systems.* 8(5), 535-550. doi: 10.1109/91.873577.

MacVicar-Whelan, P. J. (1976) Fuzzy sets for man-machine interaction. *International Journal of Man-Machine Studies*. 8(6), 687-697. doi: 10.1016/S0020-7373(76)80030-2.

Maldonado, Y. & Castillo, O. (2012) Genetic design of an interval type-2 fuzzy controller for velocity regulation in a DC motor. *International Journal of Advanced Robotic Systems*. 9, 1-8. doi: 10.5772/51188.

Mallick, A. K. & Mukhopadhyay, A. (2018) Different Schemes for Improving Fuzzy Clustering Through Supervised Learning. In: *2nd International Conference on Computational Intelligence, Communications, and Business Analytics, July 27-28, 2018, Kalyani, India.* pp. 155-164.

Mandal, A. K. (2014) *Introduction to Control Engineering: Modeling, Analysis and Design*. India, New Age International Publishers.

Mendel J. M. & John R. I. (2002) Type-2 fuzzy sets made simple. *IEEE Transactions on Fuzzy Systems.* 10(2), 117-127.

Mendel, J. M. & Wu, D. (2010). Perceptual Computing: Aiding People in Making Subjective Judgments. *Wiley-IEEE Press, New Jercy, USA.* ISBN: 0470478764

Mukhopadhyay, A. & Maulik, U. (2009) Towards improving fuzzy clustering using support vector machine: Application to gene expression data. *Pattern Recognition*. 42(11), 2744-2763. doi: 10.1016/j.patcog.2009.04.018.

Nafia, N., Kari, A. E., Hassan A. & Mjahed M. (2018) Robust interval type-2 fuzzy sliding mode control design for robot manipulators. *Robotics*. 7(3), 40. doi: 10.3390/robotics7030040.

Nie, M. & Tan, W. W. (2008) Towards an efficient type-reduction method for interval type-2 fuzzy logic systems. In: *2008 IEEE International Conference on Fuzzy Systems, June 1-6, 2008, Hong Kong, China.* IEEE. pp. 1425-1432.

Rahman, Z-A. S.A. (2017) Design of a fuzzy logic controller for controlling position of D.C. motor. *International Journal of Computer Engineering In Research Trends*. 4(7), 285-289.

Sankeshwari, S. S. & Chillé, R. (2019) Performance analysis of disturbance estimation techniques for robust position control of DC motor. *International Journal of Control, Automation and Systems*. 18, 486-494. doi: 10.1007/s12555-018-0838-7.

Storn, R. (2008) Differential Evolution Research – Trends and Open Questions. In: Chakraborty, U.K. (ed.) *Advances in Differential Evolution. Studies in Computational Intelligence.* Springer, Berlin, Heidelberg. vol. 143, pp. 1-31.

Şahin, İ. & Ulu, C. (2023) Altitude control of a quadcopter using interval type-2 fuzzy controller with dynamic footprint of uncertainty. *ISA Transactions*. 134, 86-94. doi: 10.1016/j.isatra.2022.08.020.

Wu, D. (2012) An overview of alternative type-reduction approaches for reducing the computational cost of interval type-2 fuzzy logic controllers. In: *2012 IEEE International Conference on Fuzzy Systems, June 10-15, 2012, Brisbane, QLD, Australia.* IEEE. pp. 1-8.

Wu, D. & Mendel, J. M. (2019) Recommendations on designing practical interval type-2 fuzzy systems. *Engineering Applications of Artificial Intelligence*. 85, 182-193. doi: 10.1016/j.engappai.2019.06.012.

Wu, D. & Tan, W. (2004) A type-2 fuzzy logic controller for the liquid-level process. In: *2004 IEEE International Conference on Fuzzy Systems, July 25-29, 2004, Budapest, Hungary.* IEEE. pp. 953-958.

Zadeh, L. (1975) The concept of a linguistic variable and its application to approximate reasoning-I. *Information Sciences*. 8(3), 199-249. doi: 10.1016/0020-0255(75)90036-5.

Zakovorotniy, A. & Kharchenko, A. (2021) Optimal speed controller design with interval type-2 fuzzy sets. In: *IEEE 2nd KhPI Week on Advanced Technology (KhPIWeek), September 13-17, 2021, Kharkiv, Ukraine*. IEEE. pp. 363-366.

Zeghlache, S., Benslimane T., Amardjia, N. & Bouguerra, A. (2017) Interval type-2 fuzzy sliding mode controller based on nonlinear observer for a 3-DOF helicopter with uncertainties. *International Journal of Fuzzy Systems*. 19, 1444-1463. doi: 10.1007/s40815-016-0226-5.

Zhou, H., Zhang, C., Tan, S., Dai, Y. & Duan, J. (2021) Design of the footprints of uncertainty for a class of typical interval type-2 fuzzy PI and PD controllers. *ISA Transactions*. 108, 1-9. doi: 10.1016/j.isatra.2020.08.009.